Some photonuclear cross sections relevant for shielding purposes

M.N. Martins
Laboratório do Acelerador Linear
Instituto de Física da Universidade de São Paulo, CP 66318, 05315-970 São Paulo, SP Brazil

This paper presents some experimental results of photonuclear cross sections which are relevant for shielding materials. Iron is a very important material in construction, largely used in structures, and nevertheless poorly studied in terms of its photonuclear properties. Below is presented a measurement of the photoproton cross section $^{56}Fe(\gamma,xp)$ (Fig. 1). These results were generated by the virtual photon analysis of electro- and electro-plus-photodisintegration data [1]. Also presented is a spectrum of the protons emitted at 90°, when the target was bombarded by 30 MeV electrons (Fig. 2).

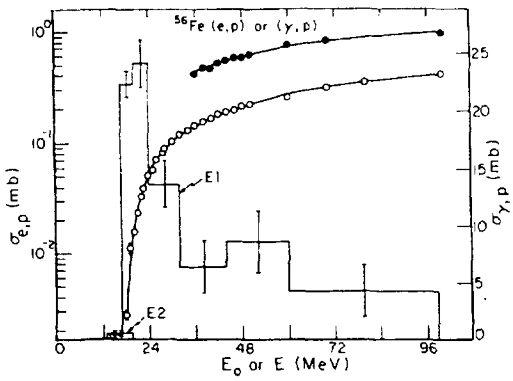

Figure 1 — Electrodisintegration cross section (open circles) and electro-plus-photodisintegration yield (full circles) of ^{56}Fe with the emission of at least one proton (left hand scale). $^{56}Fe(\gamma,xp)$ cross section (histogram, right hand scale). From Ref. [1].

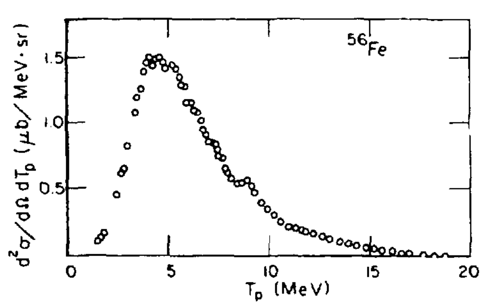

Figure 2 — Spectrum of protons emitted at 90°, when the target is bombarded by 30 MeV electrons. From Ref. [1].

Another important material in construction is Silicon, present in concrete, which is used for both structural and shielding purposes. As in most light nuclei, the photoproton cross section can be as important as the photoneutron cross sections in Silicon. As in the case of Iron, the photoproton cross sections were obtained from the virtual photon analysis of electro and electro-plus-photodisintegration data. In this case the measurement was done by detecting the residual activity of the final nucleus, so that the reaction channel is perfectly determined. Below are presented the $(\gamma,1p)$ cross sections for both ^{29}Si and ^{30}Si (Figs. 3 and 4, respectively). The relative importance of the neutron and proton channels in the photodisintegration of the Silicon isotopes can be evaluated in the figures presented below, which show a comparison between photoneutron and photoproton cross section for ^{29}Si and ^{30}Si.

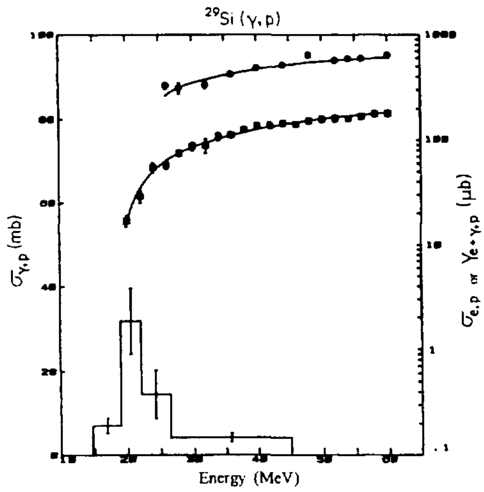

Figure 3 — ^{29}Si electrodisintegration by one proton emission (squares, right hand scale), electro-plus-photodisintegration yield (circles, right hand scale), $^{29}Si(\gamma,1p)$ cross section (histogram, left hand scale). From Ref. [2].

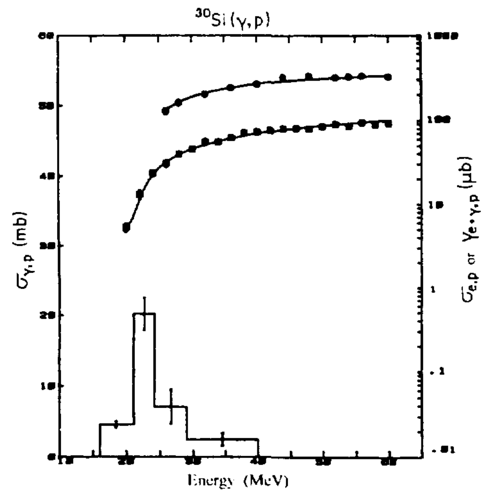

Figure 4 — Results for ^{30}Si, please see caption of Fig. 3. From Ref. [2].

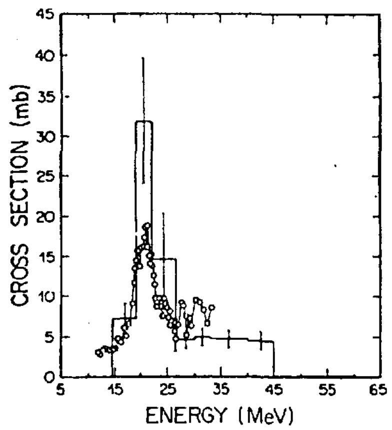

Figure 5 — Comparison between (γ,xn) (circles) and (γ,xp) (histogram) cross sections for ^{29}Si. From Ref. [2].

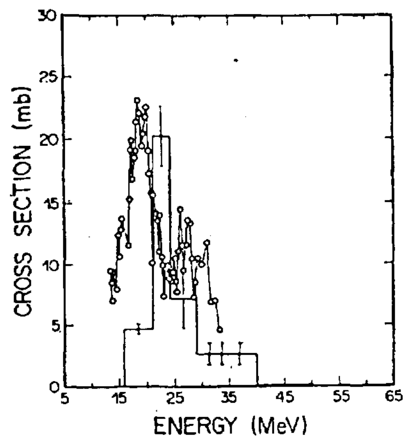

Figure 6 — Comparison between (γ,xn) (circles) and (γ,xp) (histogram) cross sections for ^{30}Si. From Ref. [2].

Table 1 shows a comparison between the integrated cross sections (up to 30 MeV) of the different channels for both ^{29}Si and ^{30}Si.

Table 1 — Comparison between ^{29,30}Si integrated photonuclear cross sections

Reaction	Threshold (MeV)	$\int \sigma dE$ (MeVmb)
^{29}Si(γ,*p*)	12.3	269(40)
^{29}Si(γ,2*p*)	21.9	8.4(24)
^{29}Si(γ,*n*)	8.50	183.0
^{29}Si(γ,*n*+γ,*np*+γ,*p*+γ,2*p*) integrated x-section: 460.4 MeVmb		
^{30}Si(γ,*p*)	13.5	151(17)
^{30}Si(γ,2*p*)	24.0	1.5(5)
^{30}Si(γ,*n*)	10.6	181.0
^{30}Si(γ,2*n*)	19.1	67.0
^{30}Si(γ,*n*+γ,*np*+γ,2*n*+γ,*p*+γ,2*p*) integrated x-section: 400.5 MeVmb		

References

[1] W.R. Dodge, R.G. Leicht, E. Hayward and E. Wolynec, Phys. Rev. **C24** (1981) 1952-1960.
[2] J.F. Dias, M.N. Martins and E. Wolynec, Phys. Rev. **C42**(1990)1559-1563.